Reliable Silicon Photonic Light Source Using Curved Distributed Feedback Lasers

Nanxi Li,[1, 2,*], Purnawirman,[1] Gurpreet Singh,[1] Emir Salih Magden,[1] Michele Moresco,[1] Thomas N. Adam,[3] Gerard Leake,[3] Douglas Coolbaugh,[3] Jonathan D. B. Bradley,[1,4] and Michael R. Watts[1]

[1]*Photonic Microsystems Group, Research Laboratory of Electronics, Massachusetts Institute of Technology, 77 Massachusetts Avenue, Cambridge, Massachusetts 02139, USA*

[2]*John A. Paulson School of Engineering and Applied Sciences, Harvard University, 29 Oxford Street, Cambridge, Massachusetts 02138, USA*

[3]*College of Nanoscale Science and Engineering, University at Albany, State University of New York, 257 Fuller Road, Albany, New York 12203, USA*

[4]*Current address: Department of Engineering Physics, McMaster University, 1280 Main Street West, Hamilton, Ontario L8S 4L7, Canada*

[*]*nanxili@mit.edu*

Abstract: We propose a curved erbium doped aluminum oxide (Al_2O_3:Er^{3+}) distributed feedback (DFB) laser for a reliable integrated photonics light source. The curved structure allows a compensation for radially varying film thickness in Al_2O_3:Er^{3+} deposition process.

OCIS codes: (130.0130) Integrated optics; (130.3120) Integrated optics devices; (140.3460) Lasers; (130.2790) Guided waves.

1. Introduction

High quality, single frequency on-chip light sources are required for many applications in silicon photonics technology [1-3]. Erbium doped aluminum oxide (Al_2O_3:Er^{3+}) distributed feedback (DFB) lasers [4-6] offer a competitive alternative to hybrid III-V silicon lasers [7-9] for high power [10], narrow linewidth [6], and thermally stable [11] integrated light sources. A CMOS-compatible waveguide design generally consists of a core silicon nitride (SiN_x) guiding layer followed by a backend-deposited active film [12-14]. Thin Al_2O_3:Er^{3+} films have been consistently grown by many research groups using a reactive co-sputtering process first described by Wörhoff et al. [15]. In a standard sputtering system, the target is mounted on a rotating platform with radially varying thickness profile from the center. Thus, a conventional straight DFB structure would experience thickness non-uniformity along the cavity.

We investigate the influence of film thickness uniformity on cavity Q and threshold power in Al_2O_3:Er^{3+} DFB lasers, and experimentally measure the thickness variation of the film across a 5-cm radius platform. We show that in a 2-cm-long Al_2O_3:Er^{3+} DFB laser even for thickness variations of < 0.5%, the cavity response can be highly distorted with significantly reduced Q. A shorter cavity would reduce the thickness variation across the DFB laser, while it limits the single pass absorption efficiency of the pump power. To improve the absorption rate, a higher doping concentration may be considered at the expense of increase in energy-transfer upconversion (ETU) and ion quenching.

In this paper, we propose a compensation scheme based on a curved DFB structure that follows the circular symmetry of the deposition system. Under the same grating parameters, an output power of 1.2 mW is achieved in a curved DFB laser, demonstrating > 6 times lower threshold power compared to a straight DFB laser. The transmission response of the curved DFB structure shows agreement with the ideal DFB structure of uniform thickness.

2. Analysis of thickness variation in straight DFB laser

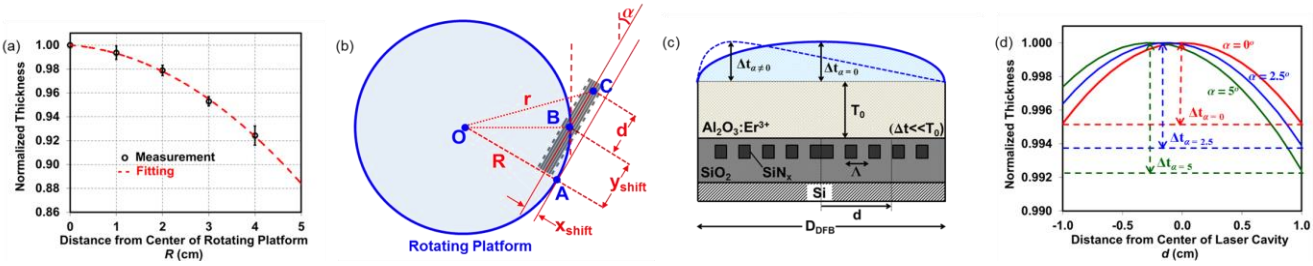

Fig. 1. (a) Measurement (black) of the Al_2O_3 film thickness fitted with a quadratic function (red) at varying distance from the center of the rotating deposition platform. (b) Diagram of the straight DFB laser placement in a radially symmetric Al_2O_3 film deposition process. (c) Illustration of thickness variation along the Al_2O_3:Er^{3+} DFB cavity. (d) Calculation of thickness profile in 2-cm-long straight DFB cavities for various tilt angles at R = 3 cm.

We measure the thickness variation of an $Al_2O_3:Er^{3+}$ film deposited in a reactive sputtering system which used 2" Er and Al sputtering targets in a confocal arrangement. The substrate is mounted on a 5-cm-radius rotating platform. After deposition, thickness measurements are performed by prism coupling at various distances R from the center of the platform. Several film depositions in the range of 1000-1500 nm are normalized as shown in Fig. 1 (a). The data is fitted with a quadratic polynomial function, estimating 12% maximum variation across the platform.

Fig. 1(b) illustrates a top view of the rotating platform with a straight DFB structure. Different parts of the DFB structure are located at varying distances r from the center O, thus inducing thickness variation along the device. Furthermore, a non-zero tilt angle α can introduce additional skew to the profile. This misalignment can also be interpreted as translational error of (x_{shift}, y_{shift}) from position where $\alpha = 0$ (point A). The thickness variation along the DFB cavity is illustrated in Fig. 1(c). The cavity with length D_{DFB} with grating period Λ is deposited with base $Al_2O_3:Er^{3+}$ thickness of T_0. The variation Δt along the cavity is skewed for $\alpha \neq 0$. The thickness variation is calculated for various tilt angles, D_{DFB} = 2 cm, and positioning at R = 3cm, as shown in Fig. 1(d). The thickness is normalized for $T_0 \approx$ 1100 nm. We obtain a small non-uniformity of 0.5%, 0.5%, and 0.8% for α = 0°, 2.5°, and 5° respectively.

3. Compensation scheme by curved DFB structure

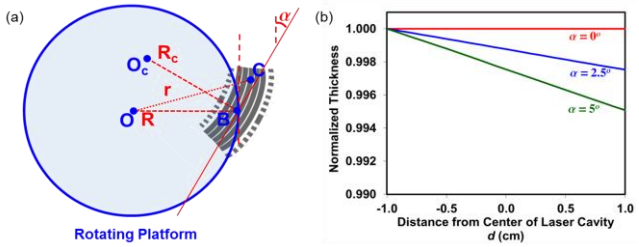

Fig. 2. (a) Diagram of the curved DFB laser placement in a radially symmetric $Al_2O_3:Er^{3+}$ film deposition chamber. (b) Calculation of thickness profile in a 2 cm long curved DFB cavity for various tilt angles at $R = R_c$ = 3cm.

To compensate for the thickness non-uniformity in the deposition, we propose a curved DFB structure that follows the circular symmetry of the platform, as shown in Fig. 2(a). By placing the curved DFB at $R = R_c$, the thickness profile can be maintained uniform throughout the cavity. The calculated thickness profile of a 2cm-long curved DFB structure at various angles shows that the profile is linear with smaller magnitude of variation, as shown in Fig. 2(b). The radial distance r as a function of position in the device d is calculated by the following formula:

$$r_{(d)}^2 = (x_{shift} + x'_{(d)}\cos\alpha + y'_{(d)}\sin\alpha)^2 + (y_{shift} - x'_{(d)}\sin\alpha + y'_{(d)}\cos\alpha)^2,$$

where (x_{shift}, y_{shift}) denotes the relative position of the DFB curvature center (point O_c) to the center of the platform (point O), and ($x'_{(d)}$, $y'_{(d)}$) is the position of a segment in the device (point C) relative to point O_c. These parameters can be calculated by the following relations:

$$x_{shift} = R - R_c\cos\alpha \qquad y_{shift} = R_c\sin\alpha \qquad x'_{(d)} = R_c\cos(d/R_c) \qquad y'_{(d)} = R_c\sin(d/R_c)$$

4. Experimental measurement of curved vs. straight DFB laser

We compare the performance of straight and curved $Al_2O_3:Er^{3+}$ DFB lasers fabricated on the same chiplet. The lasers are aligned manually at R ≈ 3 cm in the platform. We use a multi-segmented wavelength-insensitive design that consists of a silicon (Si) substrate, five SiN_x segments (thickness of 200 nm, width of 450 nm, and gap of 400 nm), enclosed by a SiO_2 layer (oxide gap of 200 nm), and $Al_2O_3:Er^{3+}$ gain film (thickness T_0 = 1100 nm). A discrete quarter phase shift is formed at the center of each cavity to produce sharp resonances at the Bragg condition. The grating is formed by additional periodic pieces on both sides with Λ = 502 nm ($\lambda_{laser} \approx$ 1590 nm). These periodic side pieces have width of 300 and gap distance of 350 nm. We use the prism coupling method to estimate a background loss of <0.1 dB/cm and dopant concentration of 1.0×10^{20} cm^{-3}.

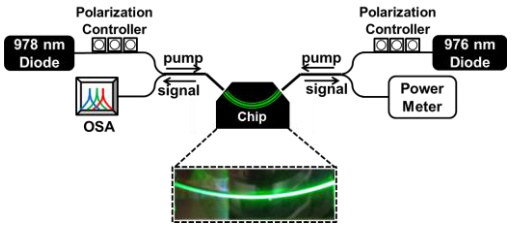

Fig. 3. Experimental setup used for curved $Al_2O_3:Er^{3+}$ DFB laser.

Fig. 3 shows the experimental setup used for the laser measurement. For the curved DFB structure, the chip edge is angle-etched to provide normally-incident coupling from a fiber. Fig. 4(a) and (b) shows the transmission measurements of the unpumped straight and curved DFB lasers, respectively. The straight DFB structure contains similar features to those calculated in the previous section, with many distorted peaks emerging in the blue-shifted wavelengths of the resonance. The resonance peak does not have a clear 3-dB width for Q estimation. The curved DFB structure shows a symmetric response, with measured $Q = 4.55 \times 10^5$.

We pump the DFB lasers from both sides using fiber pigtail laser diodes at 978 nm and 976 nm. Fig. 4 (c) shows > 6 times improvement in the threshold power for the curved DFB (P_{th} = 16 mW) compared to the straight DFB (P_{th} = 105 mW) laser, with similar slope efficiencies (0.6-0.7%). At total pump power of 188 mW, we obtain maximum output power of 1.2 mW for the curved DFB laser and less than 0.5 mW for the straight DFB laser. Lastly, Fig. 4 (d) shows the output spectra of both lasers, demonstrating a side mode suppression ratio (SMSR) of 55.7 dB for the curved DFB laser.

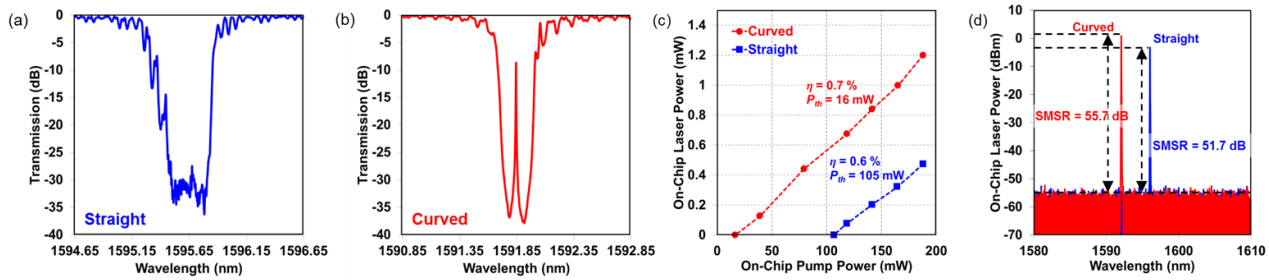

Fig. 4. Experimental measurement of straight and curved $Al_2O_3:Er^{3+}$ DFB lasers. (a) Transmission measurement of straight DFB cavity. (b) Transmission measurement of curved DFB cavity. (c) Comparison of output powers of straight and curved DFB lasers at different pump powers. (d) Optical spectra of straight and curved DFB lasers.

5. Conclusion

We investigate the influence of $Al_2O_3:Er^{3+}$ film thickness uniformity on cavity Q and threshold power in $Al_2O_3:Er^3$ DFB lasers. For thickness variations of < 0.5% in a 2-cm-long straight DFB cavity, the transmission response can be highly distorted with significantly reduced Q. We propose a compensation scheme based on a curved DFB structure that follows the circular symmetry of the $Al_2O_3:Er^{3+}$ thin film deposition system. Under the same deposition conditions and grating parameters, the curved design outperformed the conventional straight DFB structure. We achieve a slope efficiency of 0.7 %, threshold power of 16 mW, and maximum output power of 1.2 mW for the curved DFB laser. In the straight DFB laser, we obtain slope efficiency of 0.6 %, threshold power of 105 mW, and maximum output power of 0.5 mW, demonstrating > 6 times threshold power improvement.

This work is sponsored by Defense Advanced Research Projects Agency (DARPA) under E-PHI (grant no. HR0011-12-2-0007) project. N. Li is sponsored by National Science Scholarship (NSS) from the Agency of Science, Technology and Research (A*STAR), Singapore. The authors would like to acknowledge Dr. Edward Bernhardi and Dr. Joshua Conway for the helpful discussions.

6. References

[1] A. Alduino, et al., "Demonstration of a High Speed 4-Channel Integrated Silicon Photonics WDM Link with Hybrid Silicon Lasers," in *Integrated Photonics Research*, Monterey, California, 2010, PDIWI5.
[2] M. J. R. Heck, et al.,"Hybrid Silicon Photonics for Optical Interconnects," *IEEE J. of Selected Topics in Quan. Electron.*, **17**, 333-346, 2011.
[3] S. S. Sui, et al., "Sixteen-Wavelength Hybrid AlGaInAs/Si Microdisk Laser Array," *IEEE J. of Quan. Electron.*, **51**, 1-8, 2015.
[4] M. Belt, et al., "Erbium-doped waveguide DBR and DFB laser arrays integrated within an ultra-low-loss Si3N4 platform," *Opt. Express*, **22**, 10655-10660, 2014.
[5] G. Singh, et al., "Resonant pumped erbium-doped waveguide lasers using distributed Bragg reflector cavities,"*Opt. Lett.*, **41**, 1189-1192, 2016.
[6] E. H. Bernhardi, et al., "Ultra-narrow-linewidth, single-frequency distributed feedback waveguide laser in $Al_2O_3:Er^{3+}$ on silicon," *Opt. Lett.*, **35**, 2394-2396, 2010.
[7] L. Grenouillet, et al., "Hybrid integration for silicon photonics applications," *Opt. and Quan. Electron.*, **44**, 527-534, 2012.
[8] S. Stankovic, et al., "Hybrid III-V/Si distributed-deedback laser based on adhesive bonding," *IEEE Photon. Tech. Lett.*, **24**, 2155-2158, 2012.
[9] L. Tao, et al., "4-λ InGaAsP-Si distributed feedback evanescent lasers with varying silicon waveguide width," *Opt. Express*, **22**, 5448-5454, 2014
[10] E. S. Hosseini, et al., "CMOS-compatible 75 mW erbium-doped distributed feedback laser," *Opt. Lett.*, **39**, 3106-3109, 2014.
[11] M. Belt et al., "High temperature operation of an integrated erbium-doped DBR laser on an ultra-low-loss Si3N4 platform," in *Optical Fiber Communications Conference and Exhibition (OFC), 2015*, pp. 1-3.
[12] E. S. Magden, et al., "Fully CMOS-Compatible Integrated Distributed Feedback Laser with 250 ºC Fabricated Al2O3:Er3+ Gain Medium," in *CLEO* 2016 OSA Technical Digest, (Optical Society of America, 2016), paper SM1G.2.
[13] N. Li, et al., "High-power thulium lasers on a silicon photonics platform," *Opt. Lett.*, **42**, 1181-1184, 2017.
[14] Z. Su, et al., "Ultra-compact and low-threshold thulium microcavity laser monolithically integrated on silicon," *Opt. Lett.*, **41**, 5708-5711, 2016.
[15] K. Worhoff, et al., "Reliable low-cost fabrication of low-loss $Al_2O_3:Er^{3+}$ waveguides with 5.4-dB optical gain," *IEEE J. of Quan. Electron.*, **45**, 454-461, 2009.